J. Fluid Mech. (1991), *vol.* 227, *pp.* 495–508
Printed in Great Britain

Particle pressures in gas-fluidized beds

By CHARLES S. CAMPBELL AND DAVID G. WANG
Department of Mechanical Engineering, University of Southern California, Los Angeles, CA 90089-1453, USA

(Received 5 February 1990 and in revised form 3 December 1990)

The particle pressure is the surface force that is exerted due to the motion of particles and their interactions. This paper describes measurements of the particle pressure exerted on the sidewall of a gas-fluidized bed. As long as the bed remains in a packed state, the particle pressure decreases with increasing gas velocity as progressively more of the bed is supported by fluid forces. It appropriately reaches a minimum fluidization and then begins to rise again when the bed is fluidized, reflecting the agitation of the bed by bubbles. In this fully fluidized region, the particle pressure scales with the particle density and the bubble size.

1. Introduction

The particle pressure may be thought of as the force per unit area exerted on a surface by the particulate phase of a multiphase mixture and, as such, reflects the total momentum transport that can be attributed to the motion of particles and their interactions. It has a direct analogue in the kinetic theory of gases in which the pressure acting on a surface is visualized as a result of the impacts of molecules. The same picture can be applied to particle–fluid situations with the particles taking the place of molecules. The only difference between the two cases is that solid particles may, in addition to short-duration collisional impacts, transmit a force via long-duration contacts with a surface. (For example, consider a mound of particles at rest in a gravitational field. Here, the particle pressure reflects the forces exerted across their contact points and increases nearly hydrostatically with depth. This is a very different picture from the impacts of thermal molecules, yet still represents a surface force within the material.)

A term involving particle pressures often appears in theoretical models of multiphase flows. Typically, such flows are modelled as individual phase equations, in which each phase, solid or fluid, is represented by its own set of equations, each with its own associated mass, energy, pressure. The individual phase equations are then coupled together through interaction terms with the other phases in the mixture. So, in such a description of the motion of a solid–fluid mixture, one of the equations would describe the motion of the particulate phase and contain terms involving the particle pressure and other forces describing the interactions within, and the body forces acting on, the particle mass. Now, modelling the particle pressure terms has always presented a problem. In extreme cases, some theorists have ignored it as physically unsound, others have taken it to equal the fluid pressure. However, neither of these arguments seems correct in the light of the picture drawn in the last paragraph. Such extremely different viewpoints are excusable because there were no experimental measurements of particle pressure. Nonetheless, the behaviour of the particle pressure can have significant effects on the behaviour of multiphase systems. For example, Jackson (1985) and Garg & Pritchett

(1975) have shown that the stability of a fluidized bed is affected by the dependence of the particle pressure on the void fraction, reflecting the possibility that instabilities may grow or be damped through the forces transmitted within the particle phase itself.

There are alternative pictures of the particle pressure that have grown out of the fluidized bed stability literature. The early stability theories (for example Murray 1965) all indicated that a homogeneous fluidized bed should always be unstable, even though homogeneous fluidization has been experimentally obtained for beds composed of very fine particles. Many theorists have turned to the particle stress terms to try and account for this discrepancy. For example, Mutsers & Rietema (1977) envisioned the interparticle forces between small particles as being largely cohesive and, thus, able to resist the initial disturbances. Assuming that lubrication forces would keep particles from coming physically into contact, Batchelor (1988) conceived that the interparticle forces were transmitted across the intervening fluid and appeared as a force that could damp out growing instabilities within the particle phase (and, in that analysis, the major contribution to stability seemed to come from a fluid–particle interaction that forced the diffusion of particles). However, electrical conductivity data (e.g. Reed & Goldberger 1966 and Jones & Wheelock 1970) indicate that particles do actually come into contact and form bridges that convey electric current across significant portions of the bed, and which, conceivably, could also transport interparticle forces.

As the particle pressure represents the forces applied by particles, its measurement may also be of importance in industrial processes. The obvious cases would be those processes that are concerned with attrition of particles where the attrition rate would be determined by the forces applied by other particles and by the wall – and thus should be reflected in the particle pressure. Furthermore, even if they do not cause particle breakage, the forces that particles experience may work-harden their surfaces and change their physical, and possibly their chemical, attributes. Obviously, regions of largest particle pressure would be those that do the most damage and are either to be avoided or sought after depending on the desired outcome.

The only other attempt to measure the particle pressure is the recent study by Kumar, Hart & Brennen (1990) for liquid fluidized beds. They inserted a hydrophone into the wall of the bed and listened to the impacts of the particles. They calibrated their instrument by relating the output signal of the hydrophone to the impact velocity of test particles. Thus the primary measurement was the 'thermal' velocity of the impacting particles and the particle pressure was inferred from the frequency and strength of these collisions. The results showed that, with increasing fluid velocity, the particle pressure first rose, reached a maximum and then fell. This reflects two competing processes internal to the material. Increasing the fluidizing velocity increases the agitation rate of the particles and consequently increases the strength of collisions. However, at the same time, it also decreases the density within the bed, and, with it, the number of particles collisions. Eventually, the number of collisions is reduced to the point that the pressure falls despite the increased strength of individual collisions. Kumar *et al.*'s experimental technique had several drawbacks. The first was that the probe calibration was very difficult and showed a great deal of scatter which, in turn, leads to a great deal of scatter in their results. Secondly, summing all the collisions on the hydrophone was very time consuming and, consequently, very few points appear in the data. Lastly, the hydrophone could only record the thermal-like motion of the particles and could not detect long-

duration contacts, and hence, could only determine a portion of the particle pressure. (This may also be an advantage as it allows the particle pressure to be decomposed into its constituent parts.) Such is not a problem for liquid-fluidized beds, but the same method would probably not work for gas-fluidized beds in which the particles are agitated *en masse* by the passage of bubbles. Still, it represents the only existent measurements of the particle pressure.

This paper describes the measurement of particle pressure on the wall of a gas-fluidized bed using a probe that measures the sum of the particle and fluid forces and then cancels the fluid contribution. It can therefore measure the complete particle pressure in all the states of the fluidized bed, from the packed bed up to a fully slugging bed. The results are quite different than those measured by Kumar *et al.* (1990), a difference which most probably reflects the different behaviour of gas- versus liquid-fluidized beds. A preliminary report of this work appeared in Campbell (1987); however, the probe design had not been refined at that time so that the results presented there are not entirely accurate.

2. The particle pressure transducer

The particle pressure is measured using a differential pressure transducer which is illustrated in figure 1. Basically, the transducer consists of a diaphragm, flush mounted into the sidewall of the fluidized bed. Small passages about the circumference admit air, but no particles, through to the back side of the diaphragm. Thus, the front of the diaphragm experiences both gas and particle pressures and the back side experiences only gas pressure so that the net deflection of the diaphragm reflects the pressure exerted on the surface by particle interactions. Note that, owing to the time it takes enough gas to pass from the front to the rear of the diaphragm to balance the pressures, the instantaneous deflection will not necessarily correspond to the instantaneous particle pressure. However, it can be easily seen by temporal averaging of the equation of motion for a diaphragm, that the average displacement of the diaphragm will correspond to the average net force exerted on the surface. Thus, for the results presented in this paper, the signal from the pressure transducer is averaged over long periods of time to yield the average particle pressure.

The current probe is constructed of stainless steel and has a 3.8 cm (1.5 in.) diameter by 0.02 cm (0.008 in.) thick diaphragm. The displacement of the diaphragm is measured by a MTI Accumeasure capacitance probe with a 0–0.13 mm (0–0.005 in.) range. The diaphragm is thickened directly in front of the displacement transducer so as to always present a flat surface from which to take the measurement. Two passages are drilled on diametrically opposite sides of the diaphragm to permit the passages of gas through to the back side and are covered with a fine screen to keep them free of particles. During the experiments on the fluidized bed, the signal from the probe is sampled by a Scientific Solutions Labmaster data acquisition card mounted in an IBM AT which yields an average over many bubbling periods. (Samples taken from 45 to 300 s to converge to stable averages of the particle pressures.) More details of the design and testing of the transducer can be found in Campbell & Wang (1990).

The experiments are performed in the gas-fluidized bed shown schematically in figure 2. The bed is a 12.7 × 12.7 cm (5 × 5 in.) square channel, 122 cm (4 ft) tall. The air enters at the bottom through a porous plate distributor and is vented to the atmosphere through a fine screen at the top of the channel. Several ports for the pressure transducer, located 7.6, 15.2, 30.5, 45.7 and 61 cm (3, 6, 12, 18 and 24 in.)

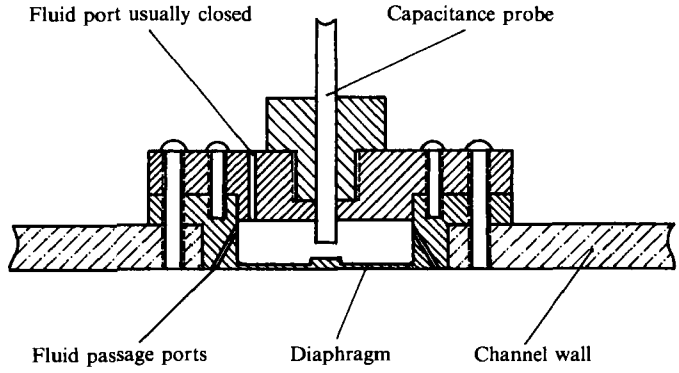

FIGURE 1. Schematic of the particle pressure transducer.

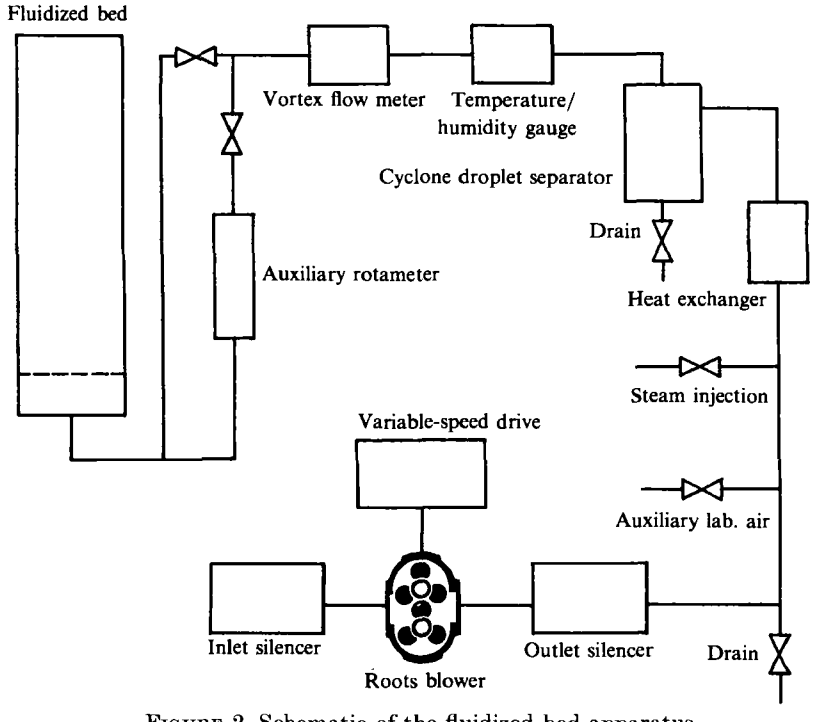

FIGURE 2. Schematic of the fluidized-bed apparatus.

from the distributor plate, were drilled in the sidewall to allow observation of any gradients of particle pressure. The gas pressure drop across the bed was monitored using a U-tube manometer attached to a pressure tap near the bottom of the channel. The void fraction in the bed was determined by a small gamma ray densitometer which consisted of a 100 μCi Cs^{137} source, collimated into a 5 cm (2 in.) diameter beam and detected by a 5×5 cm (2×2 in.) Bicron scintillation crystal detector attached to a Bicron Labtech scaler. The fluidizing air is provided by an M & D Pneumatics 3204 three-lobe Roots type blower driven by a 5 HP variable speed motor so that the flow rate may be metered by varying the speed of the blower. (An auxiliary source of air is also available from the building's compressed air supply.) Steam, from a modified pressure cooker, can be added to humidify the air to eliminate static buildup in the material inside the bed. The flow then travels through

a heat exchanger, to remove the heat of compression, and a small cyclone-type device that removes any droplets that may become entrained in the airstream from the steam injection. Afterwards, the air passes over a temperature and humidity monitoring gauge and through a Nice Instruments vortex flowmeter. As vortex flowmeters are inaccurate below a minimum flow rate, a provision has been made so that the flow may be redirected through a Dwyer RMC-SSV-123 rotameter.

3. Particle pressures in gas-fluidized beds

As a point of reference, figure 3 shows the particle pressure measured in the sidewall of a fluidized bed along with the gas-pressure drop across the bed, both plotted as a function of the superficial gas velocity. Note that, as it covers several decades, the particle pressure is plotted on a log scale while the gas pressure drop is plotted on a linear scale. These particular results were taken with the probe positioned 15 cm (6 in.) from the distributor in a 12.7 cm (5 in.) square fluidized bed. The test material was 1.2 mm glass beads carried through an entire cycle of loading to maximum fluidizing velocity and then unloading the bed completely back to zero velocity. (The properties of this and all of the materials used in this study may be found in table 1.) With zero fluidizing gas flow, the particle pressure is large, as the entire bed is supported only across interparticle contact points. Turning on the fluidizing gas causes a drop in particle pressure (and a corresponding increase in gas pressure) as progressively more and more of the bed is supported by fluid forces. The particle pressure reaches a minimum at just about the velocity where the bed is fully supported by the gas stream. A further increase in gas velocity causes the particle pressure to increase once again, presumably owing to the agitation of the bed by bubbles. As the bed begins to bubble almost immediately after minimum fluidization, the coincident rise in the particle pressure may be attributed to the agitation of the bed caused by bubble motion. But, towards the larger velocities, the bed begins to slug and, in this region, the particle pressure levels off and appears to approach a constant value.

It is somewhat interesting that the particle pressure does not go to zero at its minimum value. The particle pressure exerted on the sidewall of the bed should be some fraction of the total weight of the bed. When the bed is fully supported by fluid forces, it essentially has no weight and one might expect a zero particle pressure. However, this is not what is observed (although the measured values do approach the resolution limit of the pressure transducer). This discrepancy between intuition and observation may be attributed to a variety of causes. It is possible that, so near the minimum fluidization point, the particles in the bed are beginning to show an almost thermal like agitation (much like that observed by Kumar *et al.* 1990), which could offset some of the pressure reduction due to increasing gas flow rate. However, a more mundane possibility is that, as the particle pressure reaches its minimum at different velocities for different locations in the bed (as will be shown later in figure 7), the measured value may not reflect the actual minimum value obtained at that location but rather an average over the surface of the diaphragm.

Note that the location of this minimum provides a well-defined location that corresponds to the minimum fluidization velocity in the bed. Certainly, as it reflects the degree to which the bed is supported by fluid forces, it has much more physical significance than most methods of determination of minimum fluidization (which generally involve some sort of graphical analysis of the gas pressure-drop curve). However, all of the results in this paper use relatively large particles for which the

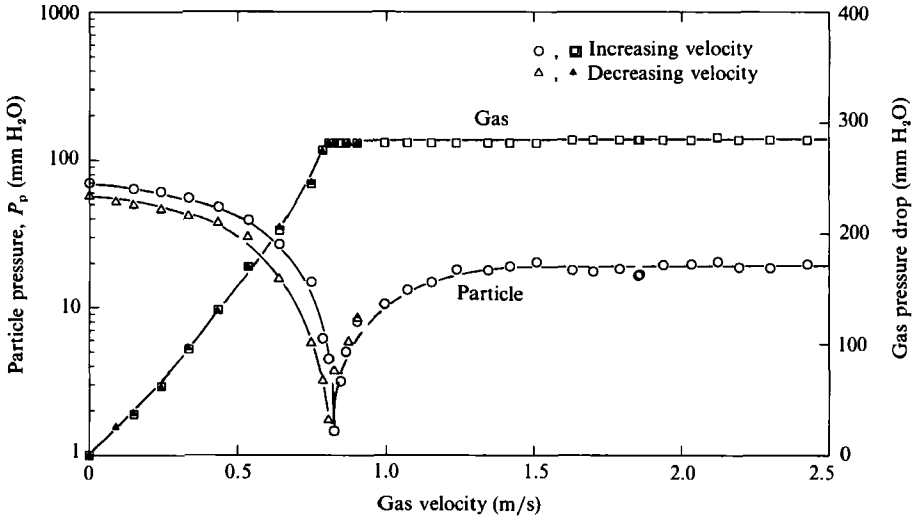

FIGURE 3. Particle pressure measurements on the sidewall of a gas-fluidized bed as a function of the superficial gas velocity. Also plotted is the gas pressure drop across the bed. The test material was 1.2 mm glass beads with an initial bed depth of 21.6 cm and the probe was mounted 15.2 cm from the distributor. Note that the particle pressure is plotted on a log scale, while the air pressure drop is plotted on a linear scale.

Material	Size (mm)	Density (kg/m^3)
Glass beads	0.50	2440
Glass beads	1.20	2440
Glass beads	2.80	2440
Steel shot	0.82	7690
Polystyrene beads	0.75	1050

TABLE 1. Test materials

minimum fluidization point and the bubbling point coincide, and it is not clear what would happen for smaller particles which have an intermediate stage where they fluidize without bubbling. Therefore, in this paper, as the particle pressure will usually be plotted by itself without the corresponding gas pressure-drop line, we will use the location of this minimum as a reference point for minimum fluidization. Points to the left of the minimum will be referred to as the packed bed state and those to the right as the fluidized state.

Unloading the superficial gas velocity from its maximum value causes the particle pressure to return along much the same path as it followed on loading. The path only begins to deviate near the point of minimum fluidization and, from that point on, returns along a lower path than it followed on loading in the region where the bed is fixed. At first, this caused great consternation since it might be caused by hysteresis in the particle pressure probe, but this pattern of behaviour is repeatable and an indication of a change in the internal structure of the packed bed. Interestingly enough, the bed returns at a smaller density and consequently a greater height. This means that a larger fraction of the bed resides above the particle pressure transducer so that, if the pressure were distributed hydrostatically, one would expect larger, not smaller, particle pressures. This implies that, on returning from a fluidized state, the forces within the bed are redistributed. The larger particle

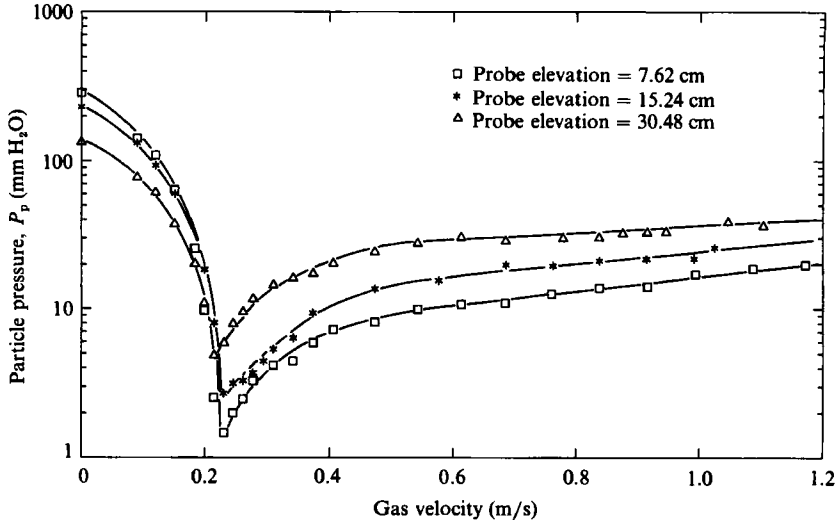

FIGURE 4. Particle pressures measured at three locations along the sidewall of the bed all of which lie within the initial packed bed. Notice that in the packed-bed region, the particle pressure decreases going upward through the bed while in the fully fluidized region, the particle pressure increases. The test material was 0.5 mm glass beads with an initial bed depth of 43.2 cm.

pressure, observed before turning on the fluidizing gas, indicates that a larger portion of the bed was supported by frictional resistance on the sidewalls. The smaller particle pressure, observed on unloading the system, indicates that more of the bed weight is distributed vertically and supported on the distributor plate. (This may be an indication that the material may form internal vertical channels to ease the passage of gas through the packed bed.) However, we noticed that tapping the side of the apparatus will cause the bed to settle, altering the internal distribution of forces and changing the path followed by the particle pressure. This indicates that the loading and unloading paths are not unique.

Figure 4 shows the particle pressure measurements for 0.5 mm glass beads, with the probe mounted at three different locations on the sidewall of the bed: 7.6, 15.2 and 30.5 cm (3, 6 and 12 in.) from the distributor. In its packed state the bed was initially about 43 cm (17 in.) deep. Before minimum fluidization, the deeper one goes in the bed, the larger the particle pressure; i.e. the particle pressure is behaving as one would expect a hydrostatic system to: the particle pressure is larger at the 7.6 cm location (the deepest in the bed) than at the 15.2 cm location, which is, in turn, larger than at the 30.5 cm location. However, beyond the fluidization point, the situation reverses, with the particle pressure increasing going upward through the bed. This may be understood by remembering that bubbles and slugs grow rapidly as they progress upward so that the higher the point in the bed the larger the particle agitation and the larger the particle pressure.

Now, all of the points shown in figure 4 were taken with the probe location that lies within the initial packed bed (which was approximately 43 cm (17 in.) deep). Figure 5 shows what happens when the probe is mounted at locations that are in the freeboard region outside the initial packed bed. Here the data for the 30.5 cm (12 in.) location are reproduced from figure 4 as a point of comparison to data taken with the probe mounted 46 and 61 cm (18 and 24 in.) above the distributor plate. At the 46 and 61 cm locations, the probe is initially uncovered so that the particle pressure is zero until the bed has expanded enough to cover the probe. In these cases, the

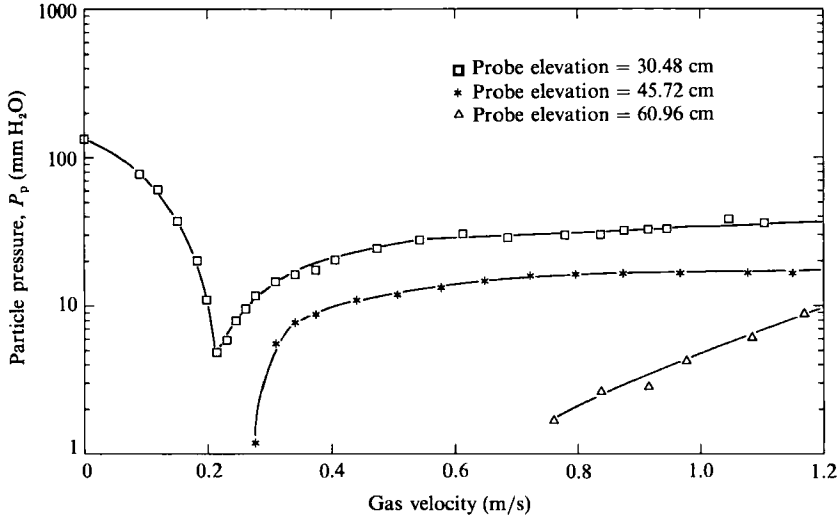

FIGURE 5. Particle pressure measured at two locations in the freeboard region above the original packed bed. For comparison, the curve from the 30.5 cm position is reproduced from figure 4. Notice that the particle pressure decreases with height outside the original packed bed. The test material was 0.5 mm glass beads with an initial bed depth of 43.2 cm.

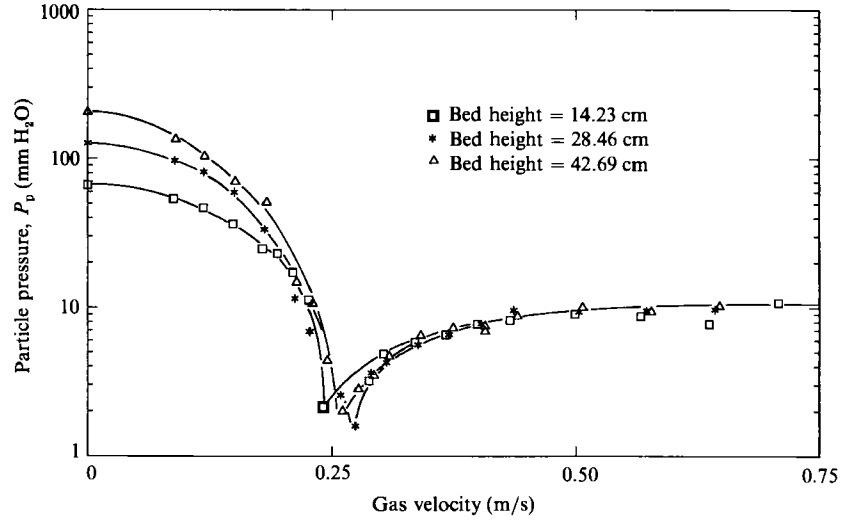

FIGURE 6. The effect of bed depth at minimum fluidization on the particle pressure. The test material is 0.5 mm glass beads and the probe was mounted 7.6 cm from the distributor.

particle pressures become smaller as the probe is moved upward. This should be expected, as when the bed is slugging it will often collapse nearly back to the packed bed state, uncovering the probe. (Note, however, that the pressures experienced at the 46 cm location are still larger than those observed at the lowest (7.6 cm) position, shown in figure 4.) In an averaged sense, it might be argued that the bed experiences an upward-pointing particle pressure gradient inside the original packed bed and a downward-pointing particle pressure gradient outside it.

The effect of bed height is shown in figure 6. (Note that the height of a fluidized bed increases with the superficial gas velocity and is thus not a well determined

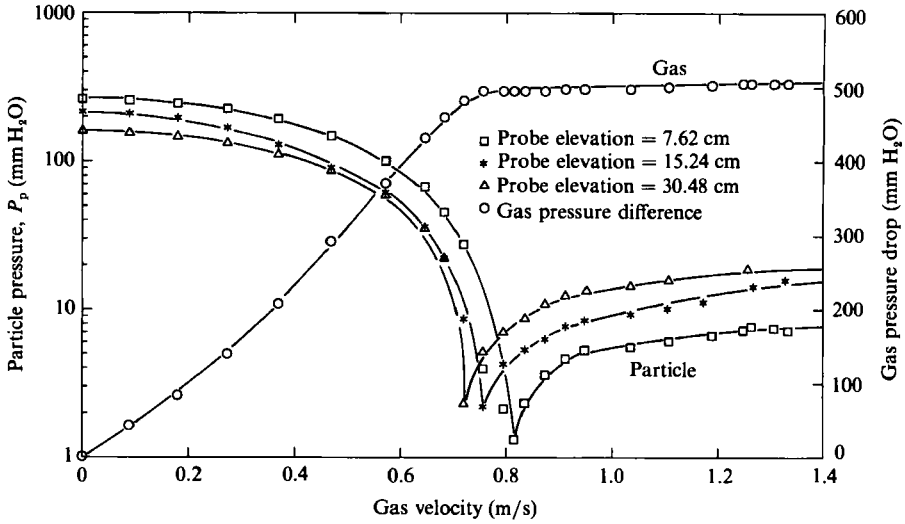

FIGURE 7. An example showing the progression of the minimum point downward through the bed as the superficial gas velocity is increased. The test material is 1.2 mm glass beads. Note that the particle pressure is plotted on a log scale, while the air pressure drop is plotted on a linear scale.

quantity; so, borrowing inspiration from the literature, we define the bed height at the minimum fluidization state.) One might expect that changing the depth of the bed over the probe position might have the same effect as mounting the probe at a lower position along the sidewall. Part of this prediction appears to be true in that, within the packed bed region, increasing the bed height above the transducer does increase the particle pressure. However, when the bed is fully fluidized, the particle pressure appears to be independent of the bed height. Thus, apparently, it is the probe's height above the distributor, and not the depth of the bed above the probe, that affects the particle pressure in the fully fluidized region.

The distribution in particle pressures throughout the bed reveals some information about the state of the bed near minimum fluidization. This is apparent in figure 4, but is easier to see with larger glass beads as the response to increased gas velocity is slower so that the effect is spread out over a much wider range. Figure 7 shows particle pressure measurements about the initial fluidization point, for 1.2 mm glass beads in a bed that is initially about 43 cm deep. These data were taken in three separate experiments, but great care was taken to prepare the beds in exactly the same way for each case. Note that the minimum point occurs at slightly higher velocities near the bottom of the bed than near the top. Furthermore, the value of the particle pressure at the minimum is smaller, the deeper one goes in the bed. Thus it appears that the bed does not reach this minimum value all at once but, instead, a front progresses down the bed over a small range of gas velocities. Most probably, this reflects the fact that bubbles first appear near the top of the bed and gradually progress downward towards the distributor with increasing gas velocity.

The next task is to try and understand the parameters – such as particle size and density – on which the particle pressure depends. As a first candidate, consider the effect of particle size demonstrated in figure 8. This shows particle pressure measurements for three sizes of glass beads, taken at the 15.2 cm probe location. As different particle sizes fluidize at different velocities, the curves would look vastly different if plotted against the fluidizing gas velocity. Instead, the particle pressure is plotted against the void fraction, ϵ, as the value of the void fraction at minimum

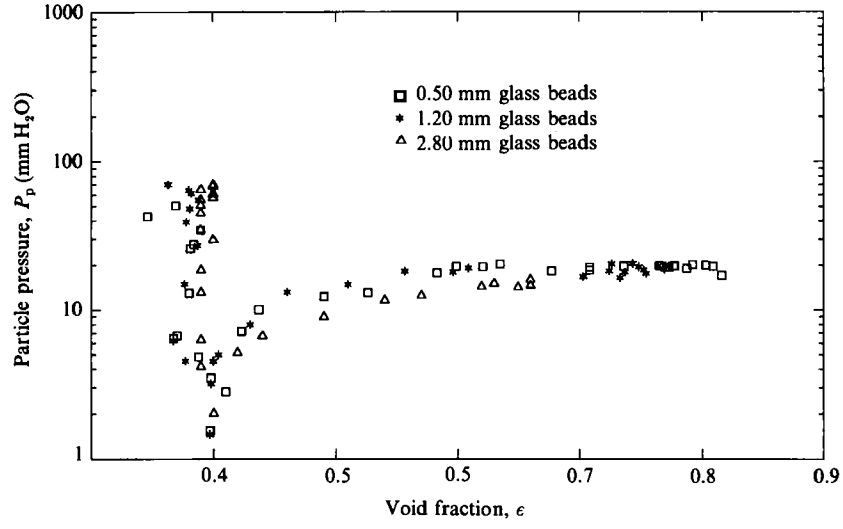

FIGURE 8. The effect of particle size on the particle pressure. This time, the data are plotted against the void fraction ϵ.

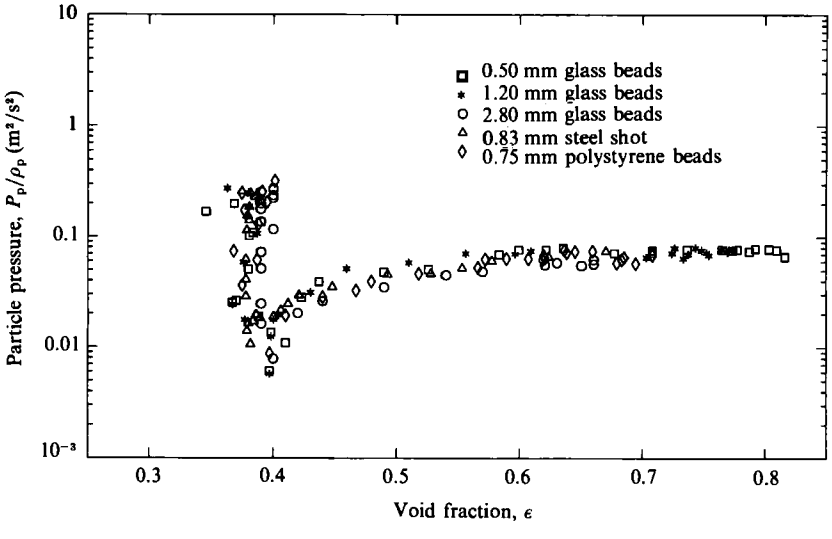

FIGURE 9. The effect of particle density on the particle pressure. Note that the particle pressure scales with the density.

fluidization is nearly independent of particle size. (Note, however, that as the void fraction increases monotonically with gas velocity, an increase in ϵ may be interpreted as an increase in the superficial gas velocity.) Plotted in this way, no significant effect of particle size can be seen, indicating that the magnitude of the particle pressures depends mostly on the material type. Note that there is scatter in the data, especially near minimum fluidization, but this may simply reflect small variations in the void fraction at minimum fluidization of the respective particle sizes.

Figure 9 shows the particle pressure measurements scaled by the solid particle density ρ_p. Once again, this is plotted as a function of the void fraction rather than the superficial gas velocity as each material type will have vastly different minimum

fluidization velocities. The results indicate that the particle pressure scales with the particle density. This is certainly true for the larger void fractions which correspond to the region where the bed is slugging, although, once again, there is variation near the minimum fluidization point probably because the different materials fluidize at slightly different void fractions.

Figure 9 indicates that we are getting close in determining the dimensional scaling of the particle pressure. To make P_p/ρ_p dimensionless would require a grouping with units of velocity squared in the denominator. However, the missing quantity is clearly not the flow velocity squared as the velocities needed to fluidize the various materials and sizes are very different. It seems more likely that the grouping has the form gL, where g is the gravitational acceleration and L is some appropriate lengthscale. Figure 8 shows that the lengthscale is not the particle size and figure 6 indicates that it cannot be the bed height.

The indications are, however, that the particle pressures in the fully fluidized region are driven by the bubble motion. So far, we have shown that the particle pressures increase moving upward through the initial packed bed (figure 4), but are independent of bed depth (figure 6) and the particle size (figure 8). All of this suggests that the proper lengthscale might be the bubble size as none of the correlations for bubble size indicate a dependence on the bed depth, the particle size or particle density except through the way they influence the minimum fluidization velocity. Furthermore, bubbles and slug will grow as they move upward through the bed which could explain the dependence on probe position shown in figure 4. Lastly, the progression of the minimum point downwards through the bed (figure 7) may indicate that the minimum simply follows the initial appearance of bubbles at progressively deeper locations. Unfortunately, we had no means with which to measure the bubble size and had to depend on correlations published in the literature. We chose the correlation of Mori & Wen (1975) as it is the only correlation that included the effect of bed width. (As our bed was rather narrow, we expected some effect of bed width on the results.) They predict

$$D_e = D_{e,\infty} - (D_{e,\infty} - D_{e,0})\, e^{-0.3x/D},$$

where

$$D_{e,0} = 0.376\,(U - U_{mf})^2$$

and:

$$D_{e,\infty} = 1.49\,[D^2(U - U_{mf})]^{0.4}.$$

Here, D_e is the equivalent bubble diameter (i.e. the diameter of a spherical bubble of the same volume as the observed bubble), $D_{e,0}$ is an estimate of the initial bubble size formed at the distributor (here we have presented the solution appropriate to porous-plate distributors), $D_{e,\infty}$ is an estimate of the 'maximum bubble size attainable by coalescence', x is the distance above the distributor, D is the equivalent bed diameter, U is the superficial gas velocity and U_{mf} is the minimum fluidization velocity. Notice that this correlation is independent of particle size, density and the depth of the bed. The only problem with using this correlation is that the equivalent bubble diameter soon reaches a state where it exceeds the width of our bed. (Such a condition is generally considered to correspond to the onset of slugging.) Thus we only use this correlation when the bubble diameter is smaller than the dimensions of the bed, after which point we assume that the bed is slugging so that the bubble size equals the bed size.

The resulting dimensionless particle pressure $P_p/\rho_p g D_e$ is plotted in figure 10 as a function of the void fraction ϵ. As the bubble diameter is undefined when the bed is

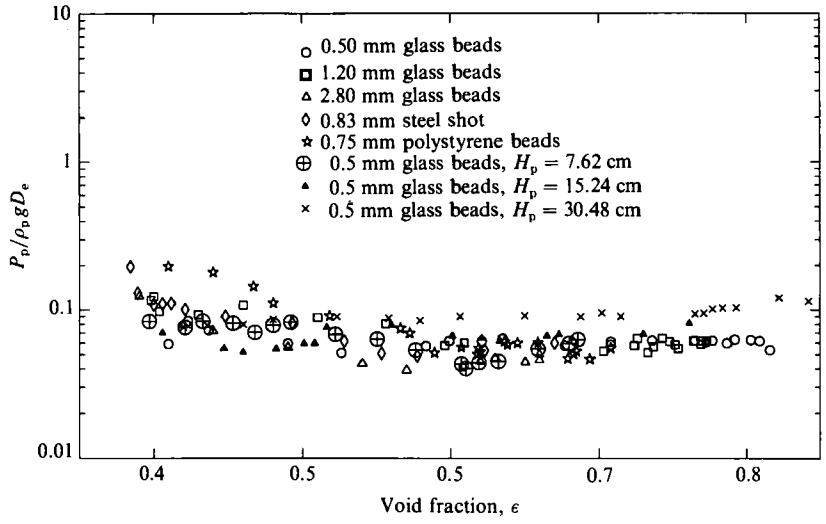

FIGURE 10. The particle pressure scaled by the particle density and the effective bubble diameter taken from the correlation of Mori & Wen (1975). Note that, with this scaling, the particle pressure is independent of everything. In particular, the initial rise in the particle is exactly modelled by the bubble growth. Here, H_p refers to the height of the probe above the distributor.

fixed, only the points after minimum fluidization are included in this plot. It appears that, when plotted this way, $P_p/\rho_p g D_e$ is nearly constant and equal to 0.08. Especially interesting is the fact that the rise in particle pressure that occurs right after minimum fluidization is well accounted for. We therefore conclude that the particle pressure in a gas-fluidized bed scales with the bubble diameter. This reflects the fact that, when fully fluidized, the bubbles are driving the internal agitation of the bed, a manifestation of which is the particle pressure exerted on the sidewall.

You might notice in figure 10 that there is some scatter in the data when the bed is slugging. This is due to the assumption above that the bubble diameter in this regime equals the bed size. This is a common assumption although it is clearly false as the volume of a slug will grow as it moves upward through the bed. The effect of this on the particle pressure is evident in our earlier observation (shown in figure 4) that the particle pressure increases slightly going upward through the bed, even when the bed is slugging. Thus, one would expect that, as we do not take this growth into account in the above scaling, the data taken in the slugging region with the probe at the 7.6 cm location would have slightly lower pressure than at the 15.2 cm location which in turn is slightly lower than at the 30.5 cm location. Exactly this behaviour is apparent in the scatter that occurs at large void fraction in the above figure. It does not, however, explain the scatter at smaller densities, which may be simply excused as a reflection of the inaccuracies inherent in the Mori & Wren correlation, or it could reflect physical phenomena, such as the pressure generation due to thermal-like motions of individual particles that are also not accounted for in the above scaling.

But notice also that the $P_p/\rho_p g D_e$ scaling explains why the particle pressure appears to approach a constant value at the higher velocities when the bed is slugging. Even though the slug size is not equal to the effective diameter of the bed, the bed size does limit the growth of slugs, thus effectively putting a cap on the largest particle pressures that can be realized. Another thing to note is that bubble

velocities scale as $(gD_e)^{\frac{1}{2}}$, indicating that the above expression is equivalent to saying that the particle pressure scale with the square of the bubble velocity. Thus, this dependence on bubble size reflects both the amount of material moved by a bubble (which should be related to the bubble size) and the velocity of the motion. One must remember, however, that these are all time-averaged quantities, so that the above scaling must also account for the frequency of bubble passage.

4. Conclusions

This paper has described measurements of the particle pressure exerted on the sidewall of a gas-fluidized bed. All the results show the same characteristic behaviour. At zero superficial gas velocity, the particle pressure is large as all of the pressure is supported across interparticle contacts. Turning on the gas flow reduces the particle pressure on the walls as progressively more of the material is supported by fluid forces. The particle pressure reaches a minimum at the point where the bed is fully supported, and, with a further increase in gas velocity, bubbles appear and the particle pressure begins to rise again owing to the agitation of the bed by bubbles.

When the bed is fully fluidized, the particle pressure appears to be dominated by the bubble motion and the particle density. A series of tests revealed that, in the fully fluidized region, the particle pressure varies as

$$\frac{P_p}{\rho_p g D_e} = \text{constant} \approx 0.08,$$

D_e was determined in a rather *ad hoc* manner using the correlation of Mori & Wen (1975) until the bubble diameter equalled the effective diameter of the fluidized bed, after which it was assumed to be constant and equal to the average equivalent bed diameter. But, despite the obvious deficiencies of the model, all of the data collapsed nearly to a point when plotted as above. In particular, the initial growth in the particle pressure after minimum fluidization correlates with the change in bubble size.

The passage of a bubble causes large-scale agitation of the particles. In other words, as the bubble size is very much greater than a particle diameter, it causes the movement of many particle masses. This is a very different picture from the force transmission by individual impacts seen by Kumar *et al.* (1990) as the mechanism leading to the particle pressure in liquid fluidized beds. Similar behaviour may occur in the particulate regime of gas-fluidized beds before bubbles appear. However, to see such events would require performing tests on very small (less than about 100 μm diameter) test materials for which this type of probe may not be suitable as the lubrication forces between the particle and the flat wall surface may significantly slow the particle before impact. (Exactly this behaviour was encountered for small, light, particles by Kumar *et al.* 1990.) While this may give an accurate account of the particle forces on the wall, the measurements will no longer reflect the behaviour within the material. We are currently developing a probe that will overcome these difficulties. (Note that lubrication forces will probably not significantly affect the measurements in the bubbling regime. There the bubbles push blocks consisting of many particles against the diaphragm, yet the lubrication forces will be due only to those particles that actually contact the diaphragm. Consequently, one can count on the inertia of a multiparticle block to overcome the lubrication effects generated at the diaphragm by such a small fraction of its constituent particles.)

The authors would like to thank Khurram Rahman, Baruch Shahar, Dennee Martel, Suleyman Biyikli and Gan Yu for their assistance in various stages of this investigation. Funding for this work was provided by the US Department of Energy under grants DE-FG22-86PC90957 and DE-FG22-88PC88913 and the US National Science Foundation under grant MEA-8352513, for which the authors are extremely grateful. Additional funding was provided by IBM, TRW, The Ralph Parsons Foundation and The International Fine Particle Research Institute. Thanks are also due to Holly Campbell for proofreading the manuscript and to Ian and Sean for staying unusually quiet.

REFERENCES

BATCHELOR, G. K. 1988 A new theory for the instability of a uniform fluidized bed. *J. Fluid Mech.* **193**, 75–110.

CAMPBELL, C. S. 1987 A technique for determining the fluidization mechanism in horizontal slurry flow. In *Proc. Solid Transport Contractor's Review Meeting, September 17–18, 1987, Pittsburgh, Pennsylvania*, pp. 68–77. US Department of Energy, Pittsburgh Energy Technology Center.

CAMPBELL, C. S. & WANG, D. G. 1990 A particle pressure transducer, suitable for use in gas-fluidized beds. *Measurement Sci. Technol.* **1**, 1275–1279.

GARG, S. K. & PRITCHET, J. W. 1975 Dynamics of gas-fluidized beds. *J. Appl. Phys.* **46**, 4493–4500.

JACKSON, R. 1985 Hydrodynamic stability of fluid-particle systems. In *Fluidization* (ed. J. F. Davidson, R. Clift & D. Harrison), pp. 47–72. Academic.

JONES, A. L. & WHEELOCK, T. D. 1970 The electrical resistivity of fluidized carbon particles: significant parameters. *Chem. Engng Prog. Symp. Series* **66** (105), 157–166.

KUMAR, S., HART, D. P. & BRENNEN, C. E. 1990 Granular pressure measurements in fluidized beds. *ASME Cavitation and Multiphase Flow Forum, June 1990, Toronto, Canada.*

MORI, S. & WEN, C. Y. 1975 Estimation of bubble diameters in gaseous fluidized beds. *AIChE J.* **21**, 109–115.

MURRAY, J. D. 1965 On the mathematics of fluidization. Part 1. Fundamental equations and wave propagation. *J. Fluid Mech.* **21**, 465–493.

MUTSERS, S. M. P. & RIETEMA, K. 1977 The effect of interparticle forces on the expansion of a homogeneous gas-fluidized bed. *Powder Technol.* **18**, 239–248.

REED, A. K. & GOLDBERGER, W. M. 1966 Electrical behavior in fluidized beds of conducting solids. *Chem. Engng Prog. Symp. Series* **62** (67), 71–75.